Robustness of free and pinned spiral waves against breakup by electrical forcing in excitable chemical media

Metinee Phantu,[1] Malee Sutthiopad,[1] Jiraporn Luengviriya,[2] Stefan C. Müller,[3] and Chaiya Luengviriya[1,*]

[1]*Department of Physics, Kasetsart University, 50 Phaholyothin Road, Jatujak, Bangkok 10900, Thailand*

[2]*Department of Industrial Physics and Medical Instrumentation, and Lasers and Optics Research Group, King Mongkut's University of Technology North Bangkok, 1518 Pibulsongkram Road, Bangkok 10800, Thailand*

[3]*Institute of Experimental Physics, Otto-von-Guericke University Magdeburg, Universitätsplatz 2, D-39106 Magdeburg, Germany*

(Received 13 August 2016; revised manuscript received 6 March 2017; published 24 April 2017)

We present an investigation on the breakup of free and pinned spiral waves under an applied electrical current in the Belousov-Zhabotinsky reaction. Spiral fronts propagating towards the negative electrode are decelerated. A breakup of the spiral waves occurs when some segments of the fronts are stopped by a sufficiently strong electrical current. In the absence of obstacles (i.e., free spiral waves), the critical value of the electrical current for the wave breakup increases with the excitability of the medium. For spiral waves pinned to circular obstacles, the critical electrical current increases with the obstacle diameter. Analysis of spiral dynamics shows that the enhancement of the robustness against the breakup of both free and pinned spiral waves is originated by the increment of wave speed when either the excitability is strengthened or the obstacle size is enlarged. The experimental findings are reproduced by numerical simulations using the Oregonator model. In addition, the simulations reveal that the robustness against the forced breakup increases with the activator level in both cases of free and pinned spiral waves.

DOI: 10.1103/PhysRevE.95.042214

I. INTRODUCTION

Spiral waves evolve in different excitable media, e.g., during CO oxidation on a platinum surface [1], cell aggregation in slime mold colonies [2], and the Belousov-Zhabotinsky (BZ) reaction [3,4]. In particular, spirals waves of action potential in heart tissues relate to some cardiac arrhythmias, such as ventricular tachycardia [5–7], which potentially develops into life-threatening ventricular fibrillation. Such a transition from ventricular tachycardia to fibrillation is associated with the spontaneous breakup of a single spiral wave of electrical activity to multiple spirals which cause an electric disorder.

Numerical simulations showed that spontaneous breakup of spiral waves in cardiac tissues is caused by conduction blocks (when a wave meets an absolute refractory zone, it fails to propagate) as found to occur in different situations as described in a detailed study by Fenton *et al.* [7]. Actually, the wave stability depends on the cellular electrophysiological properties, namely, action potential duration (APD) restitution [8] which is defined as the curve relating the present APD to the prior diastolic interval (DI) measured from the end of the previous action potential to the beginning of the next one. The wave break was observed in the case of steep APD restitution (i.e., the slope of the curve exceeds unity) at low DI [9–13].

In spite of the spontaneous emergence, wave breakups induced by the external forcing have been demonstrated in the BZ reaction under an applied electrical current [14–16]. This is due to the fact that the electrical current induces an advective motion of key ionic species in the solutions [17–19]. The wave fronts propagating to the negative electrode are decelerated and eventually stopped by the applied current stronger than a critical value [14–16,20]. Since the open ends of the broken fronts curl in and subsequently form many spiral waves, an application of very strong electrical current potentially leads to a severe situation such as fibrillation in the heart. Hagberg and Meron [16] showed that the spontaneous breakup of a wave front occurred via a subcritical pitchfork bifurcation, i.e., when the excitability parameter was varied. Furthermore, small perturbations, e.g., external applied advection, may cause wave breakup in a system close to the bifurcation point.

It is found that spiral waves are stabilized to last longer when they are pinned to obstacles, e.g., veins or scars in cardiac tissue [21]. Theoretical work [22] and simulations [23], as well as experiments using cardiomyocytes [24] and the BZ reaction [25], showed that period, speed, and wavelength of a spiral wave pinned to a circular obstacle increase with the obstacle diameter. Recently, we showed that spiral waves pinned to obstacles can be released by application of the electrical field [26–28].

In this article, we present a study of the robustness of spiral waves under an applied electric current in the BZ reaction. Two series of experiments have been performed: (I) breakup of free spiral waves at different excitability, and (II) breakup of pinned spiral waves for different obstacle size. In addition, we performed simulations using the Oregonator model [29,30] corresponding to the experiments.

II. EXPERIMENTS

A. Experimental methods

In this study, we use experimental methods similar to our previous investigations [26,27,31]: The BZ reaction is composed of $NaBrO_3$, malonic acid (MA), H_2SO_4, and ferroin, all purchased from Merck. To prevent any hydrodynamic perturbation, the reaction is embedded in a 1.0% wt/wt agarose gel (Sigma). The initial concentrations are $[NaBrO_3] = 50\,\mathrm{m}M$, $[\mathrm{MA}] = 50\,\mathrm{m}M$, and $[\mathrm{ferroin}] = 0.625\,\mathrm{m}M$, where

*fscicyl@ku.ac.th

$[H_2SO_4]$ is varied from 120 to 240 mM in the first series of experiments on free spiral waves to adjust the excitability, while $[H_2SO_4] = 160$ mM is kept constant in the second series of experiments on pinned spiral waves.

The breakup of spiral waves is studied in a uniform thin layer of the BZ reaction using a flat transparent Plexiglas reactor with the size of $100 \times 100 \times 1.0\,\mathrm{mm}^3$. An electrical current is applied via two electrodes immersed into electrolytic compartments (size of each, $25 \times 100 \times 2.0\,\mathrm{mm}^3$), located at the left and the right boundaries of the reactor. For the case of pinned spiral waves, an unexcitable obstacle made from a chemically inert plastic cylinder with a diameter of 1.5–4.5 mm and a height of 1.0 mm is set at the middle of the main volume, before the BZ solution is filled into the reactor.

The initiation of a single spiral wave is done using a two-layer strategy as in [31] for a free spiral wave and as in [26] for a pinned one. The reactor is placed in a transparent thermostating bath to remove Ohmic heat and to set the temperature at 15 °C±1 °C. The bath is put between a white light source and a color CCD camera (Super-HAD, Sony) to record the images of the medium every second with a resolution of $0.1\,\mathrm{mm\,pixel}^{-1}$.

A constant current density J is stepwise increased, until a breakup of the wave front is observed, and we define this critical value as J_{break}. For free spiral waves, a constant current density J is applied to the medium for one spiral rotation, before it is augmented by a step of $\Delta J = 5\,\mathrm{mA\,cm}^{-2}$. For pinned spiral waves, J is applied in a different way because we need to avoid the unpinning of the waves. As shown in [26,27], under sufficiently strong J, the spiral waves are released when their tips are located along the obstacle boundary facing the positive electrode (positive side). To study the breakup of a pinned spiral wave (i.e., while the spiral tip is still attached to the obstacle), J is applied to the medium only during half of each spiral rotation, and it is switched off when the spiral tip moves along the positive side of the obstacle.

B. Experimental results

In the absence of an electrical current, the free spiral waves in the BZ reaction with $[H_2SO_4]$ in the range of 120–240 mM have an isotropic structure, i.e., for each spiral wave, the wavelengths measured at different locations are very similar, as shown in Figs. 1(a) and 1(b). Under an applied electrical current, the spiral waves adopt a distorted structure as in Figs. 1(c) and 1(d) due to an acceleration and deceleration of the wave fronts moving towards the positive and negative electrodes, respectively, as well as the Doppler effect originated from an induced linear drift of the spiral tip as in [17,20].

When the density of electrical current reaches the critical value J_{break}, a segment of the innermost wave front moving towards the negative electrode is stopped and subsequently fades out, so the wave front splits into two parts as shown in Figs. 1(c) and 1(d). The breakup at other locations of the front moving towards the negative electrode occurs if the current density is further increased even by a small value of $5-10\,\mathrm{mA\,cm}^{-2}$. Therefore, J_{break} found in our experiments is a good approximation of the minimal value of the current density for inducing a breakup of the spiral waves.

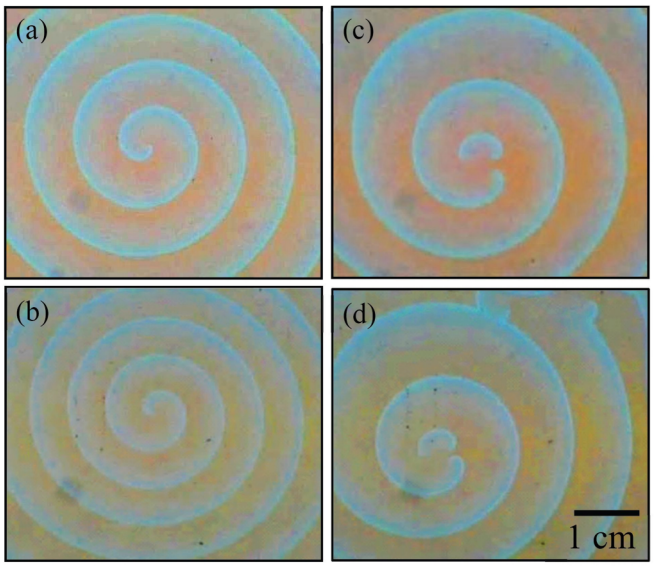

FIG. 1. Breakup of free spiral waves by an applied electrical current in the BZ reaction with $[H_2SO_4] = 160$ (top row) and 200 mM (bottom row). (a,b) spiral waves in the absence of an electrical current, while in (c,d) a wave breakup is induced by the current with $J_{\mathrm{break}} = 70$ and $105\,\mathrm{mA\,cm}^{-2}$, respectively. The positive and negative electrodes are placed on the left- and the right-hand sides, respectively.

Figure 2 summarizes the properties of free spiral waves as well as the electrical current density for the wave breakup in the BZ reaction with different excitabilities. In the absence of an electrical current, when $[H_2SO_4]$ is increased, both the wavelength λ and the wave period T decrease [Figs. 2(a) and 2(b), respectively] while both the wave speed s and the critical value of current density J_{break} increase with $[H_2SO_4]$ [Figs. 2(c) and 2(d), respectively]. Thus, the excitability has a

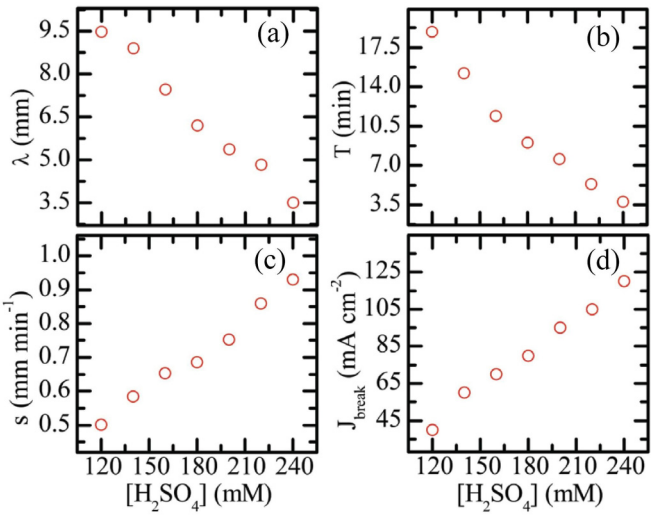

FIG. 2. Influence of excitability on the propagation and the breakup of free spiral waves in the BZ reaction: (a) wavelength λ, (b) period T, (c) speed s, and (d) critical value of the current density for breakup J_{break}.

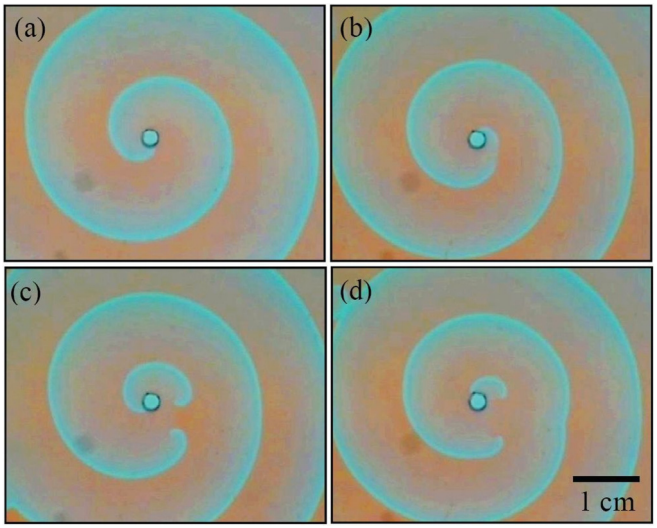

FIG. 3. Breakup of a pinned spiral wave by an applied electrical current in the BZ reaction. The obstacle diameter is 2.46 mm and positive and negative electrodes are placed on the left- and the right-hand sides, respectively. (a) The initial structure of the spiral wave is isotropic. (b) The innermost part of the wave front is stopped by the electrical current with a density of 75 mA cm^{-2}. Images (c,d) illustrate two free spiral tips evolving near the obstacle in addition to one pinned tip at 7 min and 30 min, respectively, after the applied current is switched off.

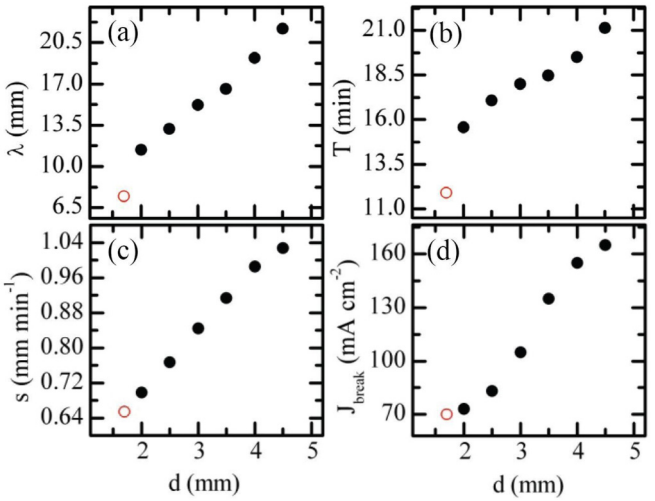

FIG. 4. Influence of obstacle diameter on the propagation and the breakup of pinned spiral waves in the BZ reaction: (a) wavelength λ, (b) period T, (c) speed s, and (d) critical value of the current density for breakup J_{break}. Open and filled circles depict free and pinned spiral waves, respectively.

similar effect on the wave speed and the forcing of the breakup of spiral waves.

It is shown in [21] that small advection (i.e., via an external forcing) can induce a wave breakup for weak excitability (located near the bifurcation point) while there is no breakup for stronger excitability. This agrees well with our finding which shows that small electrical forcing can cause a wave breakup in the BZ reaction with low excitability (low $[H_2SO_4]$). Furthermore, we show that for higher excitability the wave breakup can still occur but under a stronger electrical forcing.

The breakup of spiral waves pinned to circular obstacles with a diameter of 2.0–4.5 mm is investigated in the BZ reaction with $[H_2SO_4] = 160\,mM$, i.e., at a given excitability. Prior to the application of an electrical current, the pinned spiral waves are allowed to rotate, until they have an isotropic shape, as shown in Fig. 3(a). Similar to the case of free spiral waves, the applied current results in an anisotropic wave structure and the innermost wave front stops moving when the current density reaches the critical value J_{break}, as in Fig. 3(b). Shortly after the electrical current is switched off, the two free ends of the broken front start curling and develop into free spiral waves rotating in proximity to the obstacle while the pinned spiral tip still traces the obstacle boundary, as in Figs. 3(c) and 3(d).

The obstacles affect the intrinsic properties of the pinned spiral waves. As shown in Figs. 4(a)–4(c), the obstacles (diameter = 2.0−4.5 mm), which are larger than the free spiral core (diameter ≈ 1.7 mm), induce the spiral waves propagating with wavelength λ, wave period T, and speed s, all increasing with their diameter. Similarly, the critical value of the current density for breakup J_{break} for the pinned spiral waves is higher than that for the free spiral wave and also increases with the obstacle diameter, as shown in Fig. 4(d).

III. SIMULATIONS

A. Simulation methods

Simulations are performed using the two-variable Oregonator model which describes the dynamics of two variables u and v (corresponding to the concentrations of $HBrO_2$ and the catalyst, respectively) in the BZ reaction. The action of the electric field E applied in the x direction is added as the advection terms for both u and v:

$$\frac{\partial u}{\partial t} = \frac{1}{\varepsilon}\left(u - u^2 - fv\frac{u-q}{u+q}\right) + D_u\nabla^2 u - M_u E\frac{\partial u}{\partial x},$$
$$\frac{\partial v}{\partial t} = u - v + D_v\nabla^2 v - M_v E\frac{\partial v}{\partial x}. \quad (1)$$

The parameter values are set as in Ref. [30]: $q = 0.002$, $f = 1.4$, diffusion coefficients $D_u = 1.0$ and $D_v = 0.6$ and the ionic mobilities M_u and M_v are set to -1.0 and 2.0, respectively. The excitability of the system is adjusted via the parameter ε^{-1} from 10 to 200. In the absence of the electric field, the system supports rigidly rotating spiral waves.

An explicit Euler method with a nine-point approximation of the two-dimensional Laplacian operator and a centered-space approximation of the gradient term are used with a uniform grid space $\Delta x = \Delta y = 0.1$ system unit (s.u.) and a time step $\Delta t = 3.0 \times 10^{-3}$ time unit (t.u.), as required for numerical stability ($\Delta t \leqslant (3/8)(\Delta x)^2$ [32]). A free spiral wave is initiated as in [27].

The effect of the obstacle on the wave breakup is studied in a system with a given excitability $\varepsilon^{-1} = 100$, where the tip of the free spiral waves (without obstacles) rotates around a circle of 0.9 s.u. in diameter. A completely unexcitable circular area

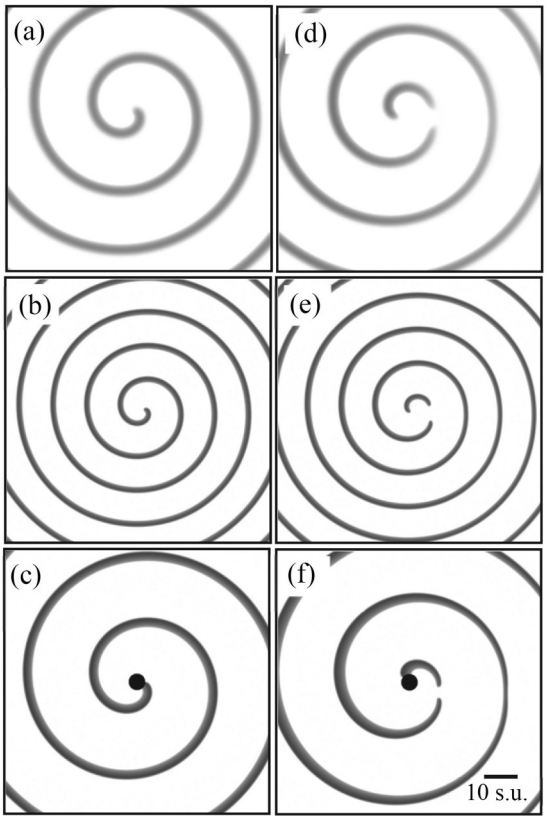

FIG. 5. Breakup of free and pinned spiral waves in the Oregonator model. (a,b) Free spiral waves at different excitability $\varepsilon^{-1} = 10$ and 100, respectively. (c) A spiral wave pinned to circular obstacle (diameter 5.0 s.u.) and $\varepsilon^{-1} = 100$. (d–f) Breakups of the spiral waves in (a–c) due to the critical electric field $E_{\text{break}} = 0.300$, 0.850, and 1.710, respectively. The field E is pointing to the right of the images.

with a diameter between 2 and 10 s.u. is set as the obstacle with no-flux boundaries as described in [27].

B. Simulation results

Figure 5 illustrates examples of spiral wave images in the simulations where the intensity (the darkness) of the spiral front corresponds to the value of the activator u. In the absence of the electric field, the front is darker at higher ε^{-1} [compare Figs. 5(a) and 5(b)] while, at a given ε^{-1}, the obstacle causes an increment of the intensity of the pinned spiral wave [Fig. 5(c)] compared to the free spiral wave [Fig. 5(b)]. In the same manner as in the experiments, a wave breakup in the simulations occurs under a sufficiently high electric field E_{break}. In all cases [e.g., Figs. 5(d)–5(f)], the innermost front, which moves in the same direction as the vector E (pointing to the negative electrode), is forced to stop and a front breakup occurs.

The effect of the excitability on the properties of free spiral waves and the wave breakup by the electric field are shown in Fig. 6. When ε^{-1} is increased, both the wavelength λ [Fig. 6(a)] and the wave period T [Fig. 6(b)] decrease, while the speed s [Fig. 6(c)] and the critical electric field E_{break} [Fig. 6(d)] increase. Thus, the experimental results in Fig. 2 are reproduced by the simulations.

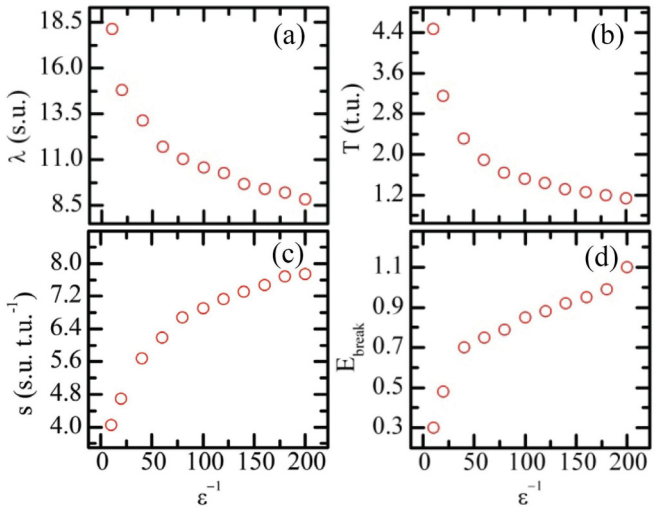

FIG. 6. Influence of excitability on (a) wavelength λ, (b) period T, (c) speed s, and (d) critical density of the field E_{break} of free spiral waves in the Oregonator model.

Figure 7 shows the simulation results of spiral waves pinned to circular obstacles with a diameter 2.0–10.0 s.u., i.e., larger than the free spiral core (diameter = 0.9 s.u.) at a given $\varepsilon^{-1} = 100$. The wavelength λ, wave period T, speed s, and critical field for breakup E_{break} of pinned spiral waves are larger than those of the free spiral waves and they increase with the obstacle diameter. Therefore, both the effects of the excitability and of the obstacle size on the intrinsic properties of spiral waves as well as the critical value of the electrical forcing for breakup, as found in the experiments (Figs. 2 and 4), agree well with the simulations (Figs. 6 and 7).

For deeper understanding of the robustness of spiral waves, we further analyze the front profile in the absence of the electric field. Figure 8 shows examples of activator u and inhibitor v

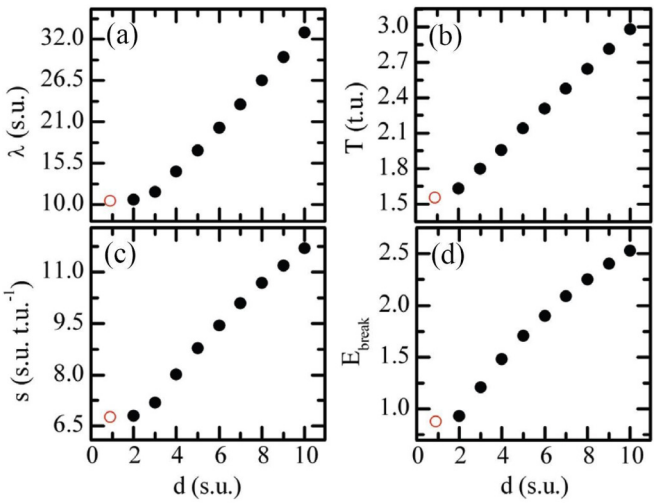

FIG. 7. Influence of obstacle diameter on the propagation and breakup of pinned spiral waves in the Oregonator model: (a) wavelength λ, (b) period T, (c) speed s, and (d) critical value of electric field for breakup E_{break}. Open and filled circles depict free and pinned spiral waves, respectively.

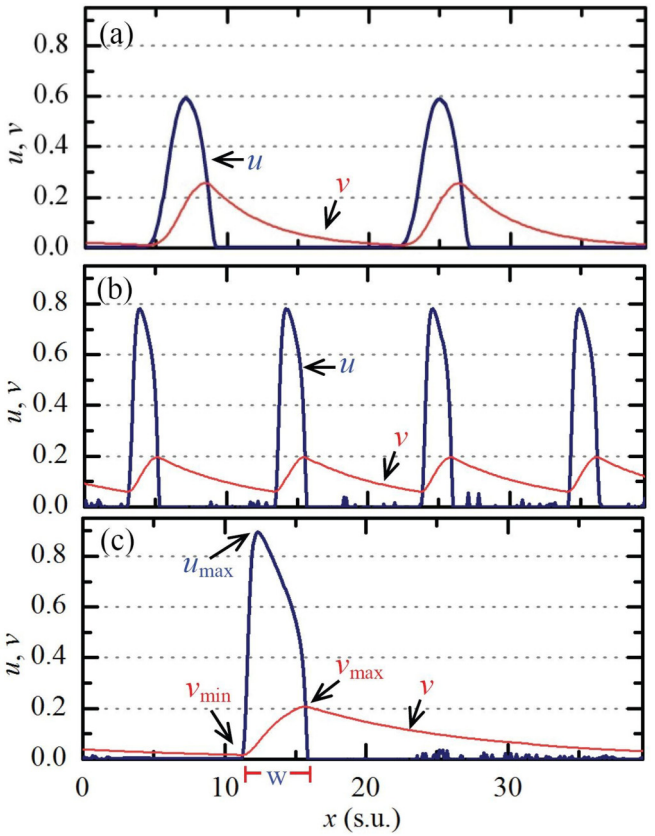

FIG. 8. Profiles of activator u and inhibitor v along a horizontal line (x) perpendicular to the fronts of free spiral waves at excitability (a) $\varepsilon^{-1} = 10$ and (b) $\varepsilon^{-1} = 100$. (c) A spiral wave pinned to a circular obstacle (diameter 10.0 s.u.) for $\varepsilon^{-1} = 100$. u_{max}, w, v_{max}, and v_{min} represent the maximum of u, the wave width, the maximum of v, and the minimum of v, respectively.

values along a horizontal line at the middle height of the system ($x = 0$–40, $y = 40$). Both u and v profiles of free spiral waves are affected by the excitability [compare Figs. 8(a) and 8(b)]. For a given excitability, the obstacle also changes the profiles [see Figs. 8(b) and 8(c)].

To specify the effect of excitability and obstacle size on the profiles, we measure the maximal u (u_{max}), the wave width (w), the maximal v (v_{max}), and the minimal v (v_{min}), as shown in Fig. 9. Note that the minimal u is about zero in all cases. When ε^{-1} is increased, u_{max} and v_{min} increase but w and v_{max} decrease [see Figs. 9(a)–9(d)]. For a given excitability, when the obstacle diameter d is increased, u_{max}, w, and v_{max} increase. However, v_{min} decreases, as shown in Figs. 9(a′)–9(d′).

IV. DISCUSSION AND CONCLUSION

We have presented an investigation of the wave breakup by electrical forcing in the BZ reaction via two series of experiments: (I) free spiral waves for different excitability, and (II) pinned spiral waves for different obstacle size. We intentionally prepared the media which support propagating waves without spontaneous breakups (e.g., the breakups concerning the restitution [7,9–13]). The results from the experiments (Figs. 1–4) are qualitatively reproduced in simulations using the Oregonator model (Figs. 5–7). This study reveals two common features of the two types of experiments as follows: Either strengthening the excitability or enlarging the obstacle size causes (A) an increment of wave speed in the absence of electrical forcing and (B) a rise of the critical value of forcing for breakup. In contrast, the excitability affects the wavelength and the wave period of spiral waves in a way different from the obstacle size: When the excitability is increased, the wavelength and the wave period decrease. However, enlarging the obstacle causes the wavelength and the wave period to increase.

To emphasize the common features described above, we plot the critical forcing for breakup and wave speed (before forcing) for both free and pinned spiral waves in the corresponding graphs of Fig. 10. All data points lie almost on the same linear regression line for both experiments [Fig. 10(a)]

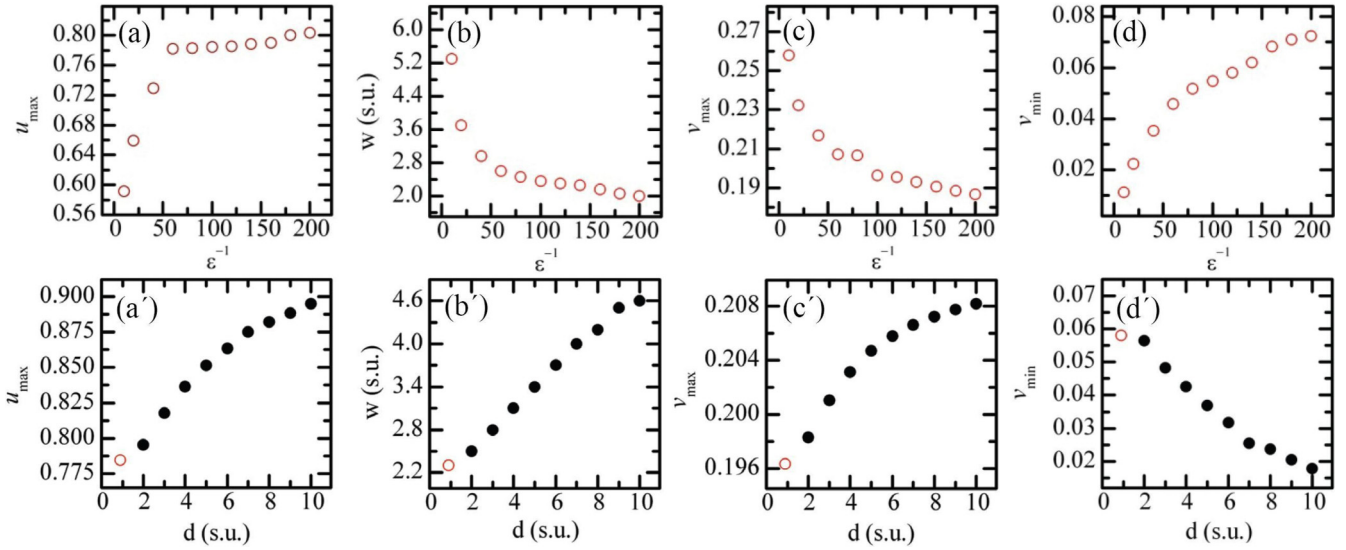

FIG. 9. (a–d) Dependence of u_{max}, w, v_{max}, and v_{min} on the excitability ε^{-1}, and (a′–d′) the obstacle diameter d, respectively. Open and filled circles depict free and pinned spiral waves, respectively.

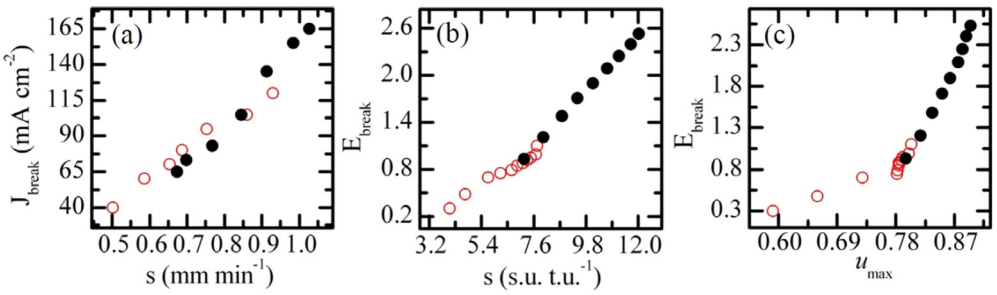

FIG. 10. Critical values of electrical forcing for breakup vs speed of wave fronts (a) in the BZ reaction and (b) in the Oregonator model and (c) u_{max} in the Oregonator model. Open and filled circles represent free and pinned spiral waves, respectively.

and simulations [Fig. 10(b)]. Thus, the wave speed is an appropriate property reflecting the robustness against a forced breakup of propagating spiral waves in general, i.e., whether in the presence of obstacles or not.

In addition, the simulations provide insight to the profiles of activator u and inhibitor v across the wave front. Surprisingly, the maximal v (v_{max}), the minimal v (v_{min}), and even the wave width w are not related to the critical forcing for breakup, since they change in different ways as the excitability and the obstacle size are varied. Only the maximal u (u_{max}) is found to connect the critical forcing [Fig. 10(c)], because they are simultaneously altered in an adjustment of the excitability or the obstacle size.

Our recent studies show that the elimination of a spiral wave, when the excitability is getting high [27] or the spiral wave is pinned to a large obstacle [26,28], becomes a tough task, since a strong forcing is required. The robustness against the forced breakup also increases with the excitability and the obstacle size, so that such a tough task of spiral elimination is still possible without any forced breakup which can lead to many spirals later. However, an application of forcing should be performed carefully; i.e., the forcing strength must not exceed the critical forcing for the wave breakup. Suitable criteria to specify such a "breakup limit," e.g., the relation between the critical forcing and the wave speed [Figs. 10(a) and 10(b)], should be elucidated in further studies. Finally, it is worth noting that the presented phenomena are expected to be observed also in other excitable media, e.g., colonies of slime mold amoebae, where the propagation of wave fronts can be modulated by an applied electric field [33].

ACKNOWLEDGMENTS

We thank the Faculty of Science, the Research and Development Institute (KURDI), the Center for Advanced Studies of Industrial Technology, and the Graduate School, Kasetsart University, and also the Office of the Higher Education Commission and King Mongkut's University of Technology North Bangkok (Contract No. KMUTNB-GOV-59-19) for financial support.

[1] S. Nettesheim, A. von Oertzen, H. H. Rotermund, and G. Ertl, J. Chem. Phys. **98**, 9977 (1993).
[2] F. Siegert and C. Weijer, J. Cell Sci. **93**, 325 (1989).
[3] A. T. Winfree, Science **175**, 634 (1972).
[4] J. Ross, S. C. Müller, and C. Vidal, Science **240**, 460 (1988).
[5] A. T. Winfree, Science **266**, 1003 (1994).
[6] R. A. Gray, A. M. Pertsov, and J. Jalife, Nature **392**, 75 (1998).
[7] F. Fenton, E. M. Cherry, H. M. Hastings, and S. J. Evans, Chaos **12**, 852 (2002).
[8] J. B. Nolasco and R. W. Dahlen, J. Appl. Physiol. **25**, 191 (1968).
[9] M. R. Guevara, G. Ward, A. Shrier, and L. Glass, IEEE Comp. Cardiol. **562**, 167 (1984).
[10] M. Courtemanche, L. Glass, and J. P. Keener, Phys. Rev. Lett. **70**, 2182 (1993).
[11] A. Karma, Chaos **4**, 461 (1994).
[12] Z. Qu, J. N. Weiss, and A. Garfinkel, Am. J. Physiol. **276**, H269 (1999).
[13] A. V. Panfilov and A. M. Pertsov, Philos. Trans. R. Soc. A **359**, 1315 (2001).
[14] J. J. Taboada, A. P. Muñuzuri, V. Pérez-Muñuzuri, M. Gómez-Gesteira, and V. Pérez-Villar, Chaos **4**, 519 (1994).
[15] H. Ševčíková, J. kosek, and M. Marek, J. Phys. Chem. **100**, 1666 (1996).
[16] A. Hagberg and E. Meron, Phys. Rev. E **57**, 299 (1998).
[17] O. Steinbock, J. Schütze, and S. C. Müller, Phys. Rev. Lett. **68**, 248 (1992).
[18] K. I. Agladze and P. De Kepper, J. Phys. Chem. **96**, 5239 (1992).
[19] A. P. Muñuzuri, V. A. Davydov, V. Pérez-Muñuzuri, M. Gómez-Gesteira, and V. Pérez-Villar, Chaos, Solitons Fractals **7**, 585 (1996).
[20] A. P. Muñuzuri, M. Gómez-Gesteira, V. Pérez-Muñuzuri, V. I. Krinsky, and V. Pérez-Villar, Phys. Rev. E **48**, R3232(R) (1993).
[21] J. M. Davidenko, A. M. Pertsov, R. Salomonz, W. Baxter, and J. Jalife, Nature **355**, 349 (1992).
[22] J. J. Tyson and J. P. Keener, Physica D **32**, 327 (1988).
[23] Y.-Q. Fu, H. Zhang, Z. Cao, B. Zheng, and G. Hu, Phys. Rev. E **72**, 046206 (2005).
[24] Z. Y. Lim, B. Maskara, F. Aguel, R. Emokpae, and L. Tung, Circulation **114**, 2113 (2006).
[25] O. Steinbock and S.C. Müller, Physica A **188**, 61 (1992).
[26] M. Sutthiopad, J. Luengviriya, P. Porjai, B. Tomapatanaget, S. C. Müller, and C. Luengviriya, Phys. Rev. E **89**, 052902 (2014).

[27] J. Luengviriya, M. Sutthiopad, M. Phantu, P. Porjai, J. Kanchanawarin, S. C. Müller, and C. Luengviriya, Phys. Rev. E **90**, 052919 (2014).

[28] P. Porjai, M. Sutthiopad, J. Luengviriya, M. Phantu, S. C. Müller, and C. Luengviriya, Chem. Phys. Lett. **660**, 283 (2016).

[29] R. J. Field and R. M. Noyes, J. Chem. Phys. **60**, 1877 (1974).

[30] W. Jahnke and A. T. Winfree, Int. J. Bifurcation Chaos **1**, 445 (1991).

[31] C. Luengviriya, U. Storb, M. J. B. Hauser, and S. C. Müller, Phys. Chem. Chem. Phys. **8**, 1425 (2006).

[32] M. Dowle, R. M. Mantel, and D. Barkley, Int. J. Bifurcation Chaos,**7**, 2529 (1997).

[33] L. Sebestikova, E. Slamova, and H. Ševčíková, Biophys. Chem. **113**, 269 (2005).